Proceedings of the Sixth International Conference on
Railway Technology: Research, Development and Maintenance
Edited by: J. Pombo
Civil-Comp Conferences, Volume 7, Paper 9.6
Civil-Comp Press, Edinburgh, United Kingdom, 2024
ISSN: 2753-3239, doi: 10.4203/ccc.7.9.6

A Wheel Wear Prediction Model Based on the Wheel-Rail Rigid Slip Considering Curve Contact Area

Y. Sun[1], M. Xing[2] and Z. Shi[3]

**[1]College of Transportation Science and Engineering,
Nanjing Tech University, China**
[2]College of Rail Transit, Wuxi University, China
**[3]Department of Industrial Engineering of Florence (DIEF),
University of Florence, Italy**

Abstract

Distribution of the wheel-rail rigid slip is a crucial parameter in predicting wheel wear. A new method based on the curve contact area is proposed to calculate the curve distributed wheel-rail rigid slip and the wheel wear distribution. The wheel wear distributions of Chinese CRH 2 EMU are calculated using the curve contact area, and those calculated using the planar contact area are compared. The simulation results indicate that the wheel-rail rigid slip based on the curve contact area is the same as that based on the plane contact area at the wheel-rail initial contact point; however, it is lower than that based on the plane contact area at other positions. Under the effect of different wheel-rail rigid slip distributions, the predicted wheel wear for the curve contact area achieves a larger depth than that for the plane contact area at the position closer to the flange; in comparison, it achieves a smaller wear depth than that for the plane contact area at the position far from the flange.

Keywords: railways, wheel wear, wheel-rail rigid slip, non-Hetzian contact, curve contact area, plane contact area.

1 Introduction

With the wheelset rolling, the wheels' wear is inevitable during the railway's vehicle operation. Wheel wear has a significant influence on the operating safety and economy of the railway; thus, wheel wear has been a problem that has attracted wide attention [1].

Several wheel wear prediction models have been proposed in previous studies to study the evolution of wheel wear [1-3]. Wheel-rail local rolling contact analysis is a crucial procedure in these wheel-wear models. The distribution of the stresses and the slip velocities inside the contact area would be calculated in local contact analysis. As a crucial parameter in local contact analysis, the distribution of the wheel-rail rigid slip has a decisive impact on the final results. In the traditional wheel wear model, the wheel-rail contact area is always assumed to be a plane. Then, the wheel-rail rigid slip distribution on the contact plane can be expressed using longitudinal, lateral, and spin creepages [4]. However, the wheel-rail contact area is essentially a curve area, which would bring specific calculation errors for the traditional wheel wear model.

The distribution of the wheel-rail rigid slip based on the curve contact area has been studied in the authors' previous study [5]. However, there is still a lack of research on how different wheel-rail rigid slip calculation methods affect the wheel wear prediction results. This study developed a new wheel wear model based on the wheel-rail rigid slip considering curve contact area. The distribution of a Chinese high-speed EMU's wheel wear is calculated using the developed wear model and the traditional model based on the plane contact area. The results of the two models are compared to show the necessity for model correction.

2 Methods

2.1 General architecture of the wheel wear prediction model

Vehicle dynamics simulation, wheel-rail local contact analysis, and wheel material wear model are critical components in a typical wheel wear prediction procedure.

In this study, a non-Hetzian contact model RNHM[5] is integral into the vehicle-track coupled dynamics model[1] to simulate the vehicle system dynamics. The global wheel-rail contact parameters, which include the wheel-rail relative displacements and wheel-rail relative velocities, can be thus obtained. A more detailed description of the vehicle-track coupled dynamics model can be found in Ref. [1]. As an improved model of the MKP+FASTSIM model, four improved strategies, which include the improvement of the wheel–rail contact angle, the wheel–rail rigid slip, the virtual penetration region reduction factor, and the ellipse-equivalent method for the nonelliptical contact area, are applied in the RNHM. A more detailed description can be found in Ref. [5].

Taking the global wheel-rail contact parameters as inputs, the local wheel-rail contact parameters, such as the contact stress and the slip velocity, can be obtained by the wheel-rail local contact analysis. The non-Hertzian contact model (RNHM) used in the vehicle-track coupled dynamics simulation is adopted in local contact analysis. Wheel–rail rigid slip is a crucial parameter for local contact analysis. A detailed description of the calculation of the wheel–rail rigid slip is described in Section 2.2.

As a variant of the famous material wear model developed by the University of Sheffield (USFD), the material wear model proposed by Yang et al. [6] is more suitable for the wheel-rail material of the Chinese high-speed EMU. Material wear depth inside the contact area can be calculated as

$$\delta_{\mathrm{w}}(x,y)=k_{\mathrm{w}}(x,y)\frac{s(x,y)}{\rho} \tag{1}$$

where k_{w} (μg/m/mm^2) is the wear rate that describes the mass (μg) of the removed material for the unit surface (mm^2) after passing through unit distance (m), $s(x,y)$ is the slip distance, and ρ is the density of the rail.

The wear rate k_{w} can be expressed as

$$k_{\mathrm{w}}(x,y)=\begin{cases}3.57\,p(x,y)\gamma(x,y), & p(x,y)\gamma(x,y)<5\\ 17.9, & 5\le p(x,y)\gamma(x,y)\le 20\\ 12.3\,p(x,y)\gamma(x,y)-228, & p(x,y)\gamma(x,y)>20\end{cases} \tag{2}$$

where $p(x,y)$ is the total tangential stress, and $\gamma(x,y)$ is the distribution of the local creep.

Accumulating wear depth inside the contact area along the rolling direction (x-direction), the wheel wear depth after the wheelset rolls a circle can be expressed as follows

$$\delta_{\mathrm{w}}(y)=\int_{x_l(y)}^{x_r(y)}\delta_{\mathrm{w}}(x,y)dx \tag{3}$$

2.2 Calculation of the wheel-rail rigid slip

Under the assumption of the planar wheel-rail contact area, the wheel-rail rigid slip distribution inside the contact area can be expressed as follows

$$\begin{cases}\bar{w}_x(x,y)=\xi_x-(y-y_{\mathrm{c}})\cdot\xi_\phi\\ \bar{w}_y(x,y)=\xi_y+(x-x_{\mathrm{c}})\cdot\xi_\phi\end{cases} \tag{4}$$

where x and y represent the longitudinal direction (wheel's rolling direction) and the lateral direction, respectively; ξ_x, ξ_y, ξ_ϕ represent the longitudinal creepage, lateral creepage, and spin creepage, respectively; x_{c} and y_{c} represent the x-coordinate and y-coordinate of the wheel–rail initial contact point, respectively.

The planar contact assumption is widely used in the previous study on vehicle dynamics simulation and wheel wear prediction. However, the wheel–rail contact area is essentially a curved area. The wheel-rail rigid slip distribution inside the actual curve contact area can be expressed as follows.

$$\begin{cases}\tilde{w}_x(x,y)=\xi_x-(y-y_{\mathrm{c}})\cdot\xi_\phi+\dfrac{\omega_{\mathrm{wy}}\Delta z_{\mathrm{wr}}(x_d(y),y)}{v_0}\\ \tilde{w}_y(x,y)=\bar{w}_y(x,y)=\xi_y+(x-x_{\mathrm{c}})\cdot\xi_\phi\end{cases} \tag{5}$$

where ω_{wy} is the angular velocities of the wheel-rail surfaces about the y-axis; $x_d(y)$ represents the location of the 'contact trace'; v_0 is the wheelset rolling speed; Δz_{wr}

represents the normal distance between the actual contact curve and the assumed contact plane, which can be written as

$$\Delta z_{\mathrm{wr}}(x,y)=\frac{z_{\mathrm{w}}(x,y)+z_{\mathrm{r}}(x,y)}{2}-\frac{z_{\mathrm{w}}(x_{\mathrm{c}},y_{\mathrm{c}})+z_{\mathrm{r}}(x_{\mathrm{c}},y_{\mathrm{c}})}{2} \tag{6}$$

where z_{w} and z_{r} represent the z-coordinates of the wheel and rail surfaces, respectively.

More detailed description of the calculation of the wheel–rail rigid slip can be found in Ref. [5].

3 Results

To study the effect of the curve distribution of the wheel-rail rigid slip on the wheel wear, a wheelset running on a straight line at a constant speed with wheelset lateral displacement Y_{w} ranged between -6 mm~6 mm is simulated. Only the wheelset rolling velocity is considered, while the wheelset velocities of the vertical motion, lateral motion, yaw angle, and roll angle are ignored. The rail is assumed to be fixed without any motion. A constant wheel-rail normal force of 73.5 kN is adopted. The wheel profiles include the standard LMA profile and a worn LMA profile. LMA is a widely used wheel in Chinese high-speed EMU, the worn LMA profile measured from a used wheel of a high-speed EMU with a running distance of 83, 000 km. The rail profile is Chinese CHN 60.

The wheel-rail longitudinal rigid slip distribution at the position of the contact trace calculated by using the plane contact area (Eq.(4)) and curve contact area (Eq.(5)) are compared, and the results for the contact between LMA&CNH 60 and worn-LMA&CNH 60 are given in Figs.1~2, respectively. In Figs.1~2, the solid line represents the results of the curve contact area, while a dashed line marks the results for the plane contact area.

The longitudinal rigid slips in Figs.1~2 show a linear distribution along the Y-axis for the plane contact area. In contrast, they show a non-linear distribution along the Y-axis for the curve contact area. The longitudinal rigid slip calculated by using two methods is the same at the location of the wheel-rail initial contact point. Meanwhile, the longitudinal rigid slip at other locations obtained by the curve contact area is slightly smaller than that obtained by the plane contact area. This is because the wheel is a concave-shaped surface, and the curvature center of the wheel profile is located outside the wheels, which makes the wheel-rail combined curvature center point to the outside of the wheels.

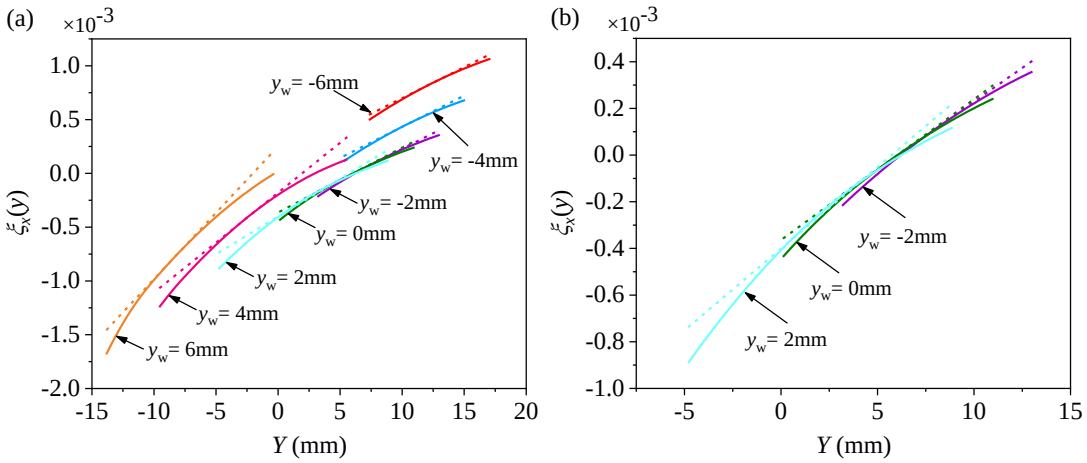

Figure 1: Comparison of the longitudinal rigid creepage calculated using the plane contact area and curve contact area for the contact between standard LMA and CNH 60. (a) Global drawing, (b) partial enlarged drawing.

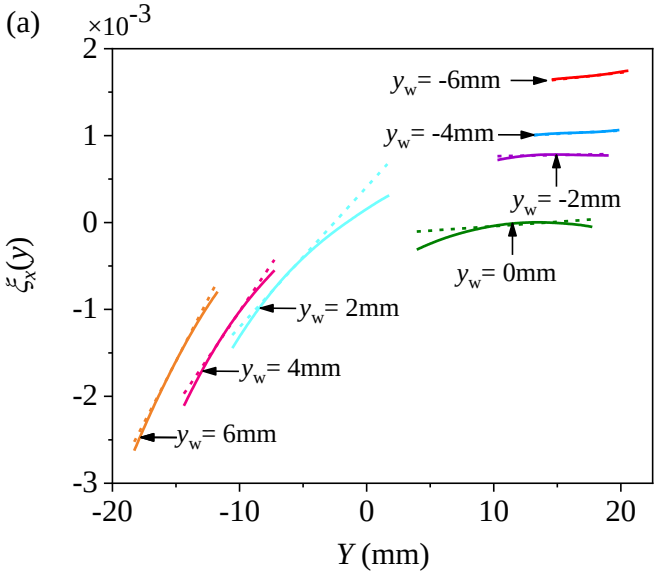

Figure 2: Comparison of the longitudinal rigid creepage calculated using the plane contact area and curve contact area for the contact between worn LMA and CNH 60.

Under the effect of the different longitudinal rigid slip distribution of Figs.1-2, the wheel wear distribution after the wheelset rolling a circle calculated by two methods are compared in Figs. 3-4. It can be observed from Fig. 3 that when the wheelset lateral displacement y_w is small (close to 0 mm), the wheel wear depth is relatively small. However, there is an evident increase in the wheel wear depth with the increase of the absolute wheelset lateral displacement. When the wheelset lateral displacement is small (y_w=-6 mm and y_w =-4 mm), the wear depth for the curve contact area is slightly smaller than that for the plane contact area; when the wheelset lateral displacement is large (y_w=4 mm and y_w =6 mm), the wear depth for curve contact area is slightly larger than that for plane contact area; when wheelset lateral displacement is close to zero (y_w=-2 mm~2 mm), the wear depth at the position close to the wheel flange for curve contact area is slightly larger than that for plane contact area. In contrast, the opposite

phenomenon occurs at the position far from the flange. It can be concluded from Fig. 1 and Fig. 3 that the wheel wear depth is in proportion to the absolute value of the longitudinal rigid slip. Similar results can also be found in the results for the worn wheel in Fig. 4. Compared with the results of the standard LMA wheel, the wear depth is significantly larger for the worn LMA wheel. The difference in the wear depth for the two methods is not evident for large absolute wheelset lateral displacement; however, as shown in Fig. 4b, the difference is evident when absolute wheelset lateral displacements relative is small.

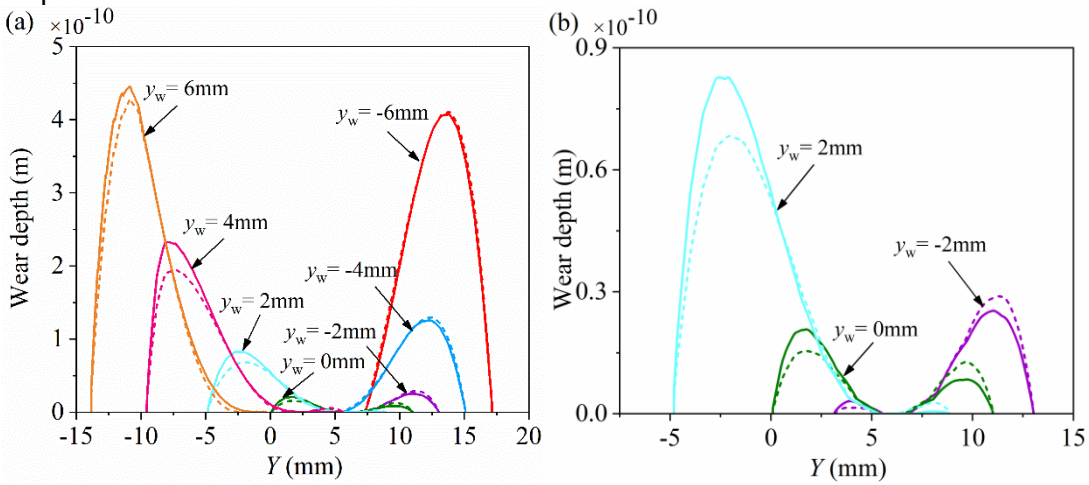

Figure 3: Comparison of the wheel wear distribution calculated using the plane contact area and curve contact area for the contact between standard LMA and CNH 60. (a) Global drawing, (b) partial enlarged drawing.

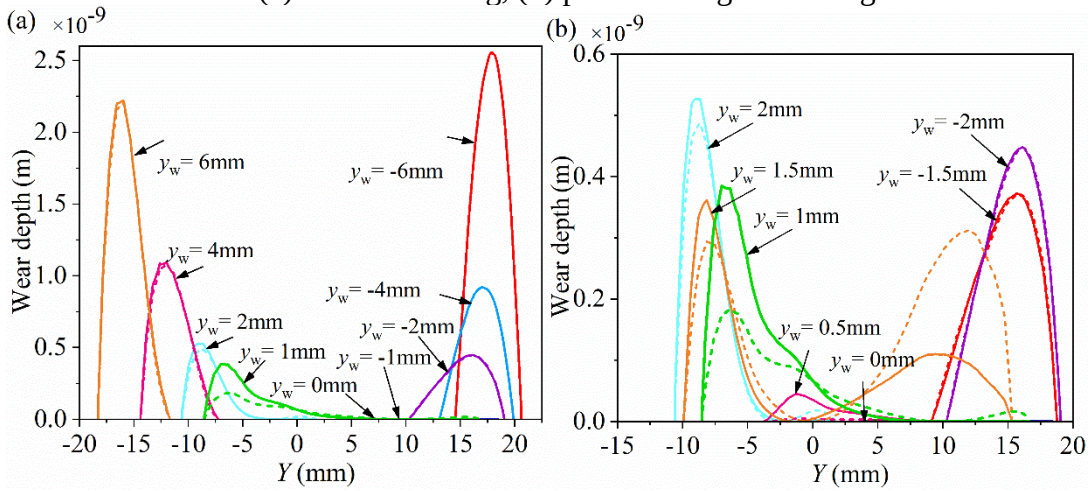

Figure 4: Comparison of the wheel wear distribution calculated using the plane contact area and curve contact area for the contact between worn LMA and CNH 60. (a) Global drawing, (b) partial enlarged drawing.

To further illustrate the influence of the curve distribution of the wheel-rail rigid slip on wheel wear prediction in actual vehicle operation. The wheel wear when a Chinese CRH2 EMU running on a straight line with the speed of 300 km/h is simulated by using the above two methods. In the simulation, the track irregularities are the

measured data of a Chinese high-speed railway. Two-wheel profiles and the rail profile are the same as those adopted in the above analysis.

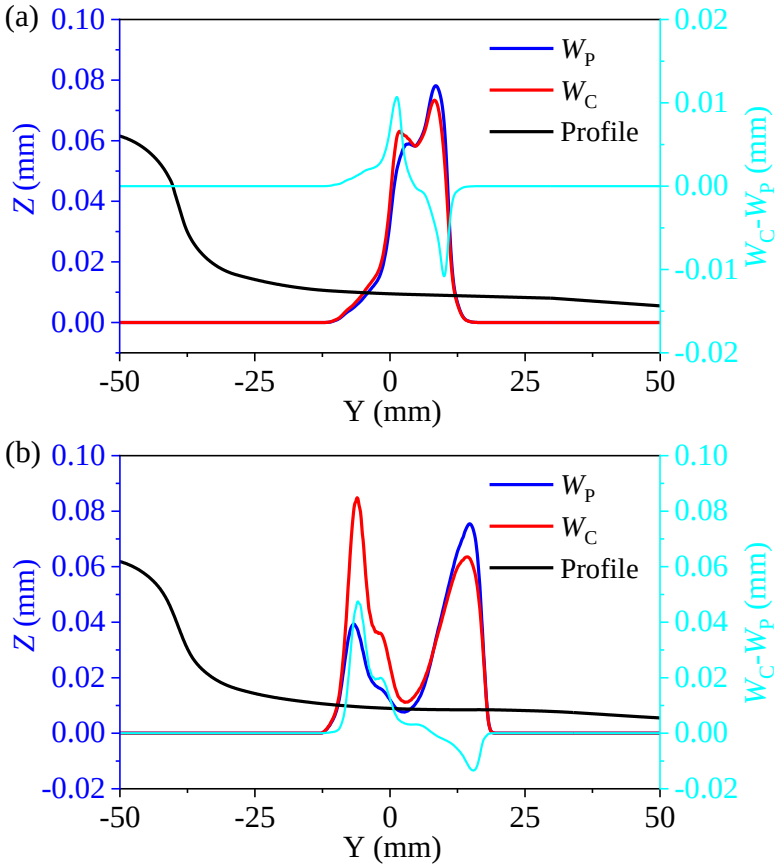

Figure 5: Comparison of the wheel-wear distribution calculated by the contact plane WP and contact curve WC. (a) Standard LMA wheel, (b) worn LMA wheel.

Figure 5 shows the wheel wear distribution when the vehicle travels 10,000 km. In the figure, W_P and W_C represent the results calculated by using the plane contact area and curve contact area, respectively.

As shown in Fig. 5(a), the wheel wear distributions for the standard LMA wheel calculated by the two methods are close. Relative to the plane contact area W_P results, the wear depth calculated using the curve contact area W_C is slightly more prominent at the position close to the flange, and it is slightly smaller at the position far away from the flange. The difference in the wheel wear between the two methods is similar to the results of the dependent contact conditions shown in Fig. 3, which indicates that the concave-down distribution of the longitudinal rigid slip in Fig. 1 is responsible for these differences.

It can be observed from Fig. 5(b) that the difference between W_P and W_C for worn LMA wheel is more significant than that of the standard LMA wheel shown in Fig. 5(b). Meanwhile, the characteristics of the differences for the two wheels are similar.

Taking the curve contact area W_C results as a reference, the wear depth close to the flange is underestimated under the assumption of plane contact area, and the wheel wear depth far from the position of the flange is overvalued.

4 Conclusions and Contributions

A new wheel-wear prediction model is developed considering the wheel-rail rigid slip based on the curved wheel-rail contact area. Wheel-rail rigid slip based on the curve wheel-rail contact area displays a non-linear distribution along the lateral direction, and its value is lower than that based on the planar wheel-rail contact area except the wheel-rail initial contact point. The developed wear model is applied to predict the wheel wear of a high-speed EMU. Under the effect of different methods for calculating wheel-rail rigid slip, wheel wear obtained by using the curve contact area displays a greater wear depth at the position of the flange side, while it displays a lower wear depth at the position far away from the flange side. The difference in the wear distribution calculated by the methods based on planar and curve contact area is slight for the standard wheel; however, the difference is evident for the worn wheel.

Acknowledgments

This work was supported by the National Natural Science Foundation of China [Grant No. 52202473], Basic Research Foundation of TaihuLight of China [Grant No. K20221050].

References

[1] N. Bosso, M. Magelli, N. Zampieri, "Simulation of wheel and rail profile wear: a review of numerical models", Railway Engineering Science, 30(4), 403–436, 2022.

[2] T. Jendel, "Prediction of wheel profile wear—comparisons with field measurements", Wear, 253 (1), 89-99, 2002.

[3] R. Enblom, M. Berg. "Simulation of railway wheel profile development due to wear—influence of disc braking and contact environment", Wear, 258 (7), 1055–1063, 2005.

[4] W. Zhai, "Vehicle–Track Coupled Dynamics Theory and Applications", Springer, Singapore, 2019.

[5] Y. Sun, F. Shi, et al., "Improving the robustness of non-Hertzian wheel–rail contact model for railway vehicle dynamics simulation", Multibody System Dynamics, 59, 193-237, 2023.

[6] B. Yang, L. Guo, et.al., "Simulation analysis of wheel wear based on the model of $T\gamma/A$-wear rate", Journal of Mechanical Engineering, 53(22), 101–108, 2017. (in Chinese)